Original Article

The Effect of Zinc Nanoparticles on Adult Rat Prostate Gland and the Possible Protective Role of Rutin: Histological and Biochemical Study

Heba R. Hashem and Mariam A. Amin

Department of Anatomy and Embryology, Faculty of Medicine, Ain Shams University, Egypt

ABSTRACT

Introduction: Zinc nanoparticles (ZnNPs) usage is evolving in different industrial and medical applications. However, recently nanoparticles were reported for their harmful effects. Rutin is a flavonoid that presents in plants, many veg¬etables, and fruits. It is considered a strong antioxidant.

Aim: To detect the effect of ZnNPs on the adult rat prostate gland and evaluating the possible protective effect of Rutin.

Materials and Methods: Fifty adult male albino rats were divided into four groups: Group I (control), Group II (ZnNPs group) rats received ZnNPs in a dose of 100 mg/kg via oral gavage feeding needle for 28 days. Group III (Rutin group): rats received rutin in a dose of 50 mg/kg via oral gavage feeding needle for 28 days. Group IV (ZnNPs- Rutin group): rats received Zn NPs and rutin at a dose and route as groups II, III. After 28 days, rats were weighed; blood samples were collected then sacrificed. The prostate glands were dissected and processed for histological (LM and EM), immunohistochemical, and biochemical studies with morphometric analysis.

Results: Light microscopic examination of Group II sections revealed degeneration of acini, vacuolation, and pyknotic nuclei of their lining cells. A highly statistically significant increase in thickness of the fibromuscular stroma ($P < 0.001$) in Masson Trichrome sections and a highly statistically significant increase ($P < 0.001$) in positive PCNA immunoreactions in the nuclei of epithelial cells were detected. Ultrathin sections showed vacuolations in acinar cells cytoplasm. Those findings are associated with a highly significant increase in Malondialdehyde, and Prostatic specific antigen. On the contrary, Group IV sections displayed restoration of prostatic acini arrangement with areas of hyperplasia and a statistically decrease in MDA, PSA.

Conclusion: These findings evidenced that Rutin had a natural protective role against ZnNPs induced prostatic cell injury in rats.

Received: 01 March 2021, **Accepted:** 03 April 2021

Key Words: Oxidative stress; PCNA; prostate gland; rutin; zinc nanoparticles.

Corresponding Author: Heba R. Hashem , PhD, Department of Anatomy and Embryology, Faculty of Medicine, Ain Shams University, Cairo, Egypt, **Tel.**: +20 10062 86556, **E-mail:** hebahramadan@gmail.com

ISSN: 1110-0559, Vol. 45, No.2

INTRODUCTION

Zinc is considered one of the nutritional supplements and is commonly used as a food additives. Also, it has a wide scope of application in many fields such as cosmetics, rubber, electronics, dye, sunscreens, and personal care products[1,2].

Nanotechnology is considered a new trend in the world with outstanding benefits in industrial and medical areas. This rapidly growing field has created the potential for increasing nanoparticle exposure to humans. A multitude of new products containing such particles reaches the market every year, often without thorough investigation towards their toxic tissue effects. Toxicity with such nanoparticles can affect the environment as well as human health[3,4,5]. Previous studies have mentioned that nanoparticle toxicity was much greater than large-size materials toxicity. These particles can reach the circulation and pass through the cell membrane or even the blood-brain barrier causing oxidative, inflammatory, and cytotoxic effects[1].

Nanoparticles (NPs) have been proven to cross biological barriers, including the barriers that protect the reproductive tissue[6]. Several studies have mentioned that various NPs can cross the blood-testis barrier and exhibit their toxic actions on spermatogenesis[7]. Male fertility depends on the content of the prostatic fluid secreted by the viable prostatic epithelial cells. Prostate gland inflammation can change fertility in males either directly or indirectly[8]. Previous studies proved that the administration of different doses of zinc nanoparticles (ZnNPs) for long periods tends to produce free radicals that exceed the anti-oxidative defensive ability of the body cells. This, in return, results in induced significant histopathological changes which can lead to cell death[9,10].

Rutin is a flavonol glycoside composed of the flavonol quercetin and disaccharide rutinose[11]. It is widely present in plants but its edible part is relatively rare. Also, It is found in green tea, apple, onion, buckwheat, many veg-etables, and fruits[12,13]. Moreover, Rutin is considered a strong

 DOI: 10.21608/ejh.2021.65558.1438

antioxidant that works as a scav¬enger of reactive oxygen species (ROS) and oxidizing lipid peroxidation. It has many pharmacological benefits that include anticancer, anti-mutagenic, antibacterial, antiviral, myocardial protecting, and effective in some neurodegenerative disorders[14]. It is also known to improve endothelial functions by lowering nitric oxide production in the endothelial cells[15].

Very limited studies have investigated the specific toxic effects of zinc nanoparticles (ZnNPs) on prostate gland cells. Furthermore, few research papers studied the protective relation between consumption of Rutin over such toxicity in case of inevitable exposure. Thus, the present work aimed to elaborate on the possible protective effect of Rutin against histopathological changes correlating induced by zinc nanoparticles on rat's prostate gland cells.

MATERIAL AND METHODS

Experimental animals

Fifty male Wistar albino rats, aged 14-16 weeks and weighing 200 ± 20 g, were purchased from the animal house of the Medical Research Center, Faculty of Medicine, Ain Shams University (Cairo, Egypt) and maintained in wire polypropylene cages under standard conditions (21 ± 2°C); 12 h light-dark cycle. The rats had access to water and diet ad libitum. Before the initialization of the experiment, rats were given one week for acclimatization. The experimental protocols were designed using the national guidelines approved by CARE (Committee of Animal Research Ethics) of the faculty of medicine at Ain-Shams University and following the NIH Guidelines for the Care and Use of Laboratory Animals 8th edition.

Chemicals

- **Zinc Nanoparticles (ZnNPs):** purchased from Sigma–Aldrich Co (St.Louis, MO, USA). Its Chemical Abstract Service Registration Number (CAS No) is 7440-66-6 and the product number is 578002. ZnNPs were in the form of grey nano-powder, purity ≥99% trace metals basis, and molecular weight 65.39g/mol.
- **Rutin:** Tablets 50's containing powder (Sophorae japonica Linn (flower)) 500mg from COUNTRY LIFE. /USA.

Characterization of ZnNPs (Figure 1)

Transmission Electron Microscopy (TEM) was used to evaluate the size and morphology of ZnNPs, a drop of the solution was placed on the carbon-coated copper grids and dried at room temperature[16]. Electron micrographs were obtained using (JEOLJEM-1010) transmission electron microscope at 70 kV at Electron Microscope Research Unit, The Regional Centre for Mycology and Biotechnology, Al-Azhar University, Egypt.

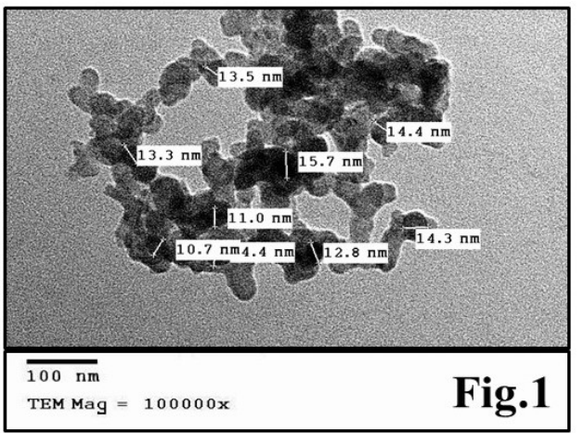

Fig. 1: Transmission electron micrograph of ZnNPs suspension showing most of the nanoparticles are spherical with an average size of 13.34± 1.6 nm. TEM X 100000

Experimental design

Each rat was weighed once per week then doses were adjusted accordingly. Rats were divided randomly into four groups as follows (ten rats/ group or subgroup).

Group I (control group): Ia: rats were not subjected to any procedure and served as a control.

Ib: rats have received 1 ml distilled water via oral gavage feeding needle, the diluting vehicle for ZnNPs, and Rutin.

Group II (ZnNPs group): rats received ZnNPs in a dose of 100 mg/kg body weight dissolved in distilled water via oral gavage feeding needle for 28 days[17].

Group III (Rutin group): rats received rutin in a dose of 50 mg/kg body weight dissolved in distilled water via oral gavage feeding needle for 28 days[13].

Group IV (ZnNPs- Rutin group): rats received ZnNPs and rutin at a dose and route like the previous groups.

Sampling and tissue Preparation

At the end of the experiment, rats of each group were weighed, fasted overnight then anesthetized by ether inhalation. Blood samples were collected from the retro-orbital plexuses. The abdominal incision was performed, and the prostate gland was dissected out and weighed then processed for histological, immunohistochemical, and tissue homogenate studies.

Relative organ weight

The prostate gland was weighed by using a sensitive portable mini digital LCD electronic scale. The relative organ weights (ROW) ratio was calculated as follows: ROW= absolute organ weight (g)/final body weight (g) x 100[18].

Histological studies

a) Light microscope studies:

The dissected prostate specimens were placed in 10 % formalin. The samples were dehydrated using a graded percentage of ethanol and then embedded in melted paraffin wax for 1 hour then form paraffin blocks. The blocks were trimmed and cut into 5-µm thick sections. Sections were stained with the following:

- Hematoxylin–Eosin (H&E)[19].
- Periodic acid Schiff reagent (PAS): for the detection of mucopolysaccharide[19,20].
- Masson Trichrome: for the detection of collagen fibers[19].

The slides were examined and photographed with the Lecia ICC50 camera.

b) Electron microscopic studies

Prostate specimens were fixed in glutaraldehyde and osmium tetroxide. The fixed parts were dehydrated and embedded in Epon 812. Semithin sections were cut less than 1 µm thick and stained with toluidine blue. These sections were examined by light microscope and used to choose the selected areas. Ultrathin sections were stained by uranyl acetate and lead citrate[19]. Transmission Electron Microscope study was performed with a JEOL JEM-1010 (Japan) at the Regional Center for Mycology and Biotechnology, Al-Azhar University, Egypt.

Immunohistochemical examination

PCNA, a marker for proliferating cells, is a rabbit polyclonal antibody (catalog number ab15497, Abcam, Cambridge, UK). The slides were incubated at 4◦C overnight with polyclonal primary antibodies. After that slides were rinsed then incubated in 0.3 % H2O2 in TBS for 15 min. Secondary antibodies (Goat antibodies, catalog number ab205718, Abcam, Cambridge, UK) was applied to the slide, diluted in TBS with 1% BSA, and incubated for 1 h at room temperature. Negative control sections were performed with the same procedure, but the primary antibody was non-immune rabbit serum[21].

The slides were examined and photographed with the Lecia ICC50 camera.

Tissue Homogenate (determination of redox status)

The tissue samples were homogenized in 0.5 ml of the serum and 0.5 ml of 30% Trichloroacetic acid (TCA). The homogenate was centrifuged at 3000 rpm for 5 min, and the supernatant was collected.

Malondialdehyde (MDA) level: Colorimetric/ Fluorometric Assay Kit, Catalog # K739-100, BioVision, USA. it is the indicator of oxidative stress and lipid peroxidation. 0.5 ml of supernatant was added to 0.5 ml of 1% thiobarbituric acid in a boiling water bath for 30 minutes followed by an ice-cold water bath for 10 minutes[22].

Samples were processed at Tissue culture & Research Center, Al-Azhar University.

Biochemical analysis for measurements of Prostatic specific antigen (PSA)

Blood samples were centrifuged at 3000 r/min for 10 min for serum separation. Serum PSA levels were measured by a mini VIDAS automate analyzer (BioM´erieux, Marcy-l' Etoile, France) using enzyme-linked immunofluorescent assay (ELISA) kits. The high levels of PSA may indicate the presence of prostate cancer and many other conditions, such as an enlarged or inflamed prostate. All blood samples were processed at Tumor Markers Oncology Research Center, Al-Azhar University.

Morphometric study

Images were analyzed using computer-based software (Leica Qwin 500; Imaging Systems, Cambridge, UK). The measurements were done in ten non-overlapping fields randomly selected in slides of each animal in each group. The following parameters were measured:

a. The mean area percent of collagen deposition using Masson trichrome stained sections at x100 magnification.

b. The mean number of PCNA positive cells at x400 magnification.

Statistical Analysis

Data were expressed as mean and standard deviation (SD) for the quantitative variable; then statistically analyzed using the Statistical Package for Social Sciences version 16 (SPSS Inc., Chicago, USA). Comparison between groups was done using ANOVA (analysis of variance) followed by the Tukey's Post Hoc test for multiple comparisons between every 2 groups. The results were considered as statistically significant when *P-value* < 0.05 and highly significant when *P-value* < 0.001.

RESULTS

During the study period (28 days), there were no signs of morbidity or mortality recorded between rats with generally good conditions.

Light and electron microscopic examination of sections of the prostate gland from groups I (control) and III (Rutin group) showed comparable findings with no detectable differences. Thus, they were represented as the control group (I) in the figures. Concerning statistical results also group III (Rutin group) showed a non-statistically significant difference in all parameters in comparison to group I ($P > 0.05$).

Histological results

1.1. Hematoxylin and eosin (H&E)

Examination of H&E stained sections of the prostate from group I (control) showed that it was formed of acini of variable sizes, containing prostatic secretion in their

lumina and lined with columnar epithelial cells having basal nuclei and resting on a basement membrane. The acini were surrounded by a stroma formed mainly of a fibromuscular capsule and septa containing smooth muscle fibers and blood vessels (Figures 2,3).

On the contrary, the examination of H&E stained sections of rat prostate from group II (ZnNPs group) revealed hyperplasia of the glandular epithelium that changes the lining to be formed of multiple layers of epithelial cells that projects into the lumen giving the form of finger-like processes (Figure 4). Some prostatic acini have marked degeneration of their lining epithelium. Some degenerated cells are shedding in the lumen and others have small pyknotic nuclei (Figure 5). Marked thickening of the connective tissue septa of the surrounding stroma containing many inflammatory cells, vacuolation, and congested blood vessel (Figures 4,5).

However, H&E stained sections of the prostate from group IV (ZnNPs-Rutin group) showed diminished nanoparticle-induced changes and appeared more or less as the control. Prostatic acini showed slight variability in size and shape (Figure 6) with small areas of hyperplasia (Figures 6,7). Fibromuscular stroma between the acini apparently decreased in thickness where is no vacuolation, or congestion in blood vessels (Figures 6,7).

1.2. Periodic acid Schiff results

Periodic acid Schiff stained sections of the rat prostate from group I (control) showed a PAS-positive reaction in the epithelial lining, prostatic secretions as well as in basement membrane (Figure 8). By contrast, sections of the prostate from group II (ZnNPs group) showed a decrease in PAS-positive reaction in the epithelial lining and basement membrane (Figure 9). Periodic acid Schiff stained sections of group IV (ZnNPs-Rutin group) showed a PAS-positive reaction in the epithelial lining and basement membrane which apparently looks like sections of control (Figure 10).

1.3. Masson trichrome results

Examination of Masson trichrome stained sections of group I (control) revealed a minimal amount of collagen fibers between the prostatic acini (Figure 11). On the other hand, sections of group II (ZnNPs group) showed an abundant amount of collagen fibers between prostatic acini and around congested blood vessels (Figure 12). However, group IV (ZnNPs-Rutin group) sections showed a few amounts of collagen fibers between prostatic acini and around blood vessels (Figure 13).

1.4. Immunohistochemical results

Immunohistochemically, prostate sections from group I (control) showed positive PCNA immunoreactions in few nuclei of the epithelial cells (Figure 14). On the contrary, the immunohistochemical sections of group II (ZnNPs group) showed intense nuclear PCNA immunoreactions in many nuclei of the lining epithelium (Figure 15). Group IV (ZnNPs- Rutin group) immunohistochemical sections showed PCNA immunoreactions in some of the nuclei of the epithelial cells (Figure 16).

1.5. Semithin results

Toluidine blue-stained sections of group I showed that the prostatic acini were lined with tall columnar cells containing basal vesicular nuclei with a prominent nucleoli. A prominent basement membrane and the fibromuscular stroma were also observed (Figure 17). Group II (ZnNPs group) toluidine blue-stained section showed hyperplasia in the glandular epithelium (Figure 18). However, the examination of sections of group IV (ZnNPs- Rutin group) revealed that the prostatic acini were lined by columnar epithelium separated by fibromuscular stroma as control. An interesting finding was the presence of mitotic figures in some nuclei (Figure 19).

1.6. Transmission electron microscopic results

Ultrathin sections of rat prostate from group I (control) showed that the prostatic acinar cells had a basal euchromatic nucleus and their cytoplasm contained rough endoplasmic reticulum, mitochondria which were surrounded by a scanty amount of collagen fibers as the basement membrane (Figure 20).

By contrast, ultrathin sections of the prostate from group II (ZnNPs group) showed that some of the acinar cells were electron-lucent with irregular nuclei and others were electron-dense with regular nuclei. Some of the irregular nuclei appeared bilobed with an irregular outline (Figure 21). Their cytoplasm contained vacuoles with electron-dense structures inside (Figures 21,22). Bundles of collagen fibers were observed with separation between the acinar cells and the basement membrane (Figure 22). Vacuolation of the cytoplasm was noticed (Figures 21,22).

On the other hand, group IV (ZnNPs -Rutin group) ultrathin sections showed some of the acinar cells were more or less as the control. All cells were of the same electron densities, but their nuclei contain euchromatin or heterochromatin. Their cytoplasm contained vacuolation and rough endoplasmic reticulum. An apparent decrease in the amount of fibrous tissue in the basement membrane (Figure 23).

Tissue homogenate results

Lipid peroxidation results in the generation of MDA which can be used as a marker of oxidative stress. MDA level in the prostate gland of rats of group II (ZnNPs group) showed a highly statistically significant increase in comparison to the group I (control) ($P < 0.001$). On the other hand, the MDA level in the prostate gland of rats of group IV (ZnNPs-Rutin group) showed a statistically significant decrease in comparison to group II ($P < 0.05$) (Histogram 1a, Table 1).

Biochemical results

Prostate-specific antigen (PSA): the mean serum level of PSA in group II (ZnNPs group) showed a highly

statistically significant increase in comparison to group I (control) ($P < 0.001$). However, in group IV (ZnNPs-Rutin group), there was a highly statistically significant decrease in comparison to group II (ZnNPs group) ($P < 0.001$) (Histogram 1b, Table 1).

Morphometric results

4.1. Relative organ weight (ROW)

ROW in group II (ZnNPs group) showed a non-statistically significant increase in comparison to the group I (control) ($P > 0.05$). On the other hand, group IV (ZnNPs -Rutin group) showed a non-statistically significant decrease in comparison to group II (ZnNPs group) ($P > 0.05$) (Histogram 2a, Table 2).

4.2. Mean area of a percent (%) of collagen fibers

The percent area of collagen fibers in group II (ZnNPs group) revealed a highly statistically significant increase in comparison to the group I (control) ($P < 0.001$). However, in group IV (ZnNPs-Rutin group) the percent area there showed a highly statistically significant decrease in comparison to group II (ZnNPs group) ($P < 0.001$) (Histogram 2b, Table 2).

4.3. The mean number of PCNA positive cells

The mean number of PCNA immunoreactive nuclei of lining epithelium in group II (ZnNPs group) showed a highly statistically significant increase in comparison to the group I (control) ($P < 0.001$) while the percent area of PCNA immunoreactive cells in group IV (ZnNPs-Rutin group) revealed a statistically significant decrease in comparison to group II (ZnNPs group) ($P < 0.05$) (Histogram 2c, Table 2).

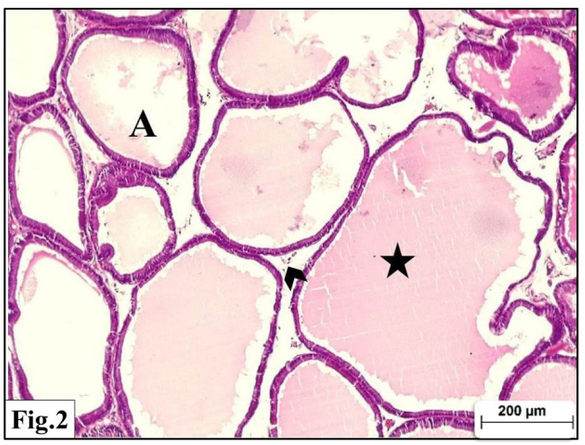

Fig. 2: A photomicrograph of a section of rat prostate gland from the control group (group I) showing prostatic acini (A) containing prostatic secretion (asterisk) in their lumen and is surrounded by fibromuscular stroma (arrowhead). H&E x100

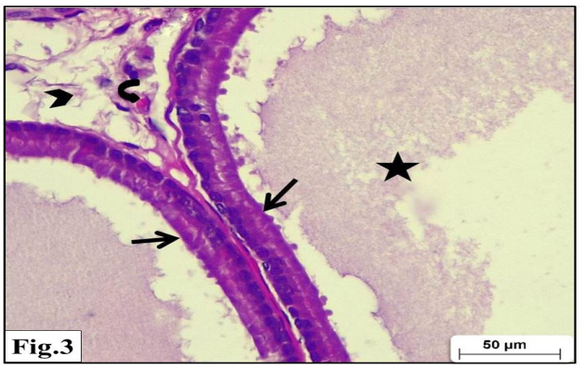

Fig. 3: A photomicrograph of a section of rat prostate gland from the control group (group I) showing parts of two adjacent prostatic acini are lined by columnar epithelium (arrow) containing prostatic secretion (asterisk) in their lumen and are surrounded by fibromuscular stroma (arrowhead) containing blood capillaries (curved arrow). H&E x400

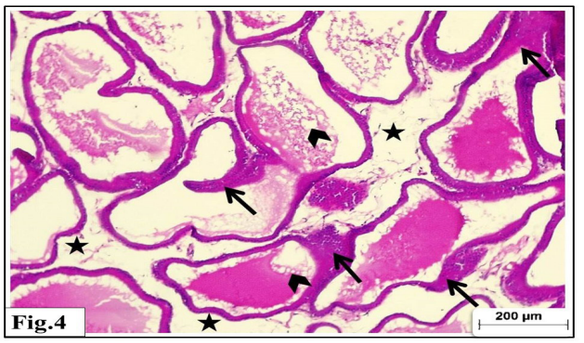

Fig. 4: A photomicrograph of a section of rat prostate gland from ZnNPs group (group II) showing distortion in prostatic acini, lined by many layers of epithelial cells (arrow), and thick stroma (asterisk) separates the acini. Notice the vacuolation in prostatic secretion (arrowhead). H&E X100

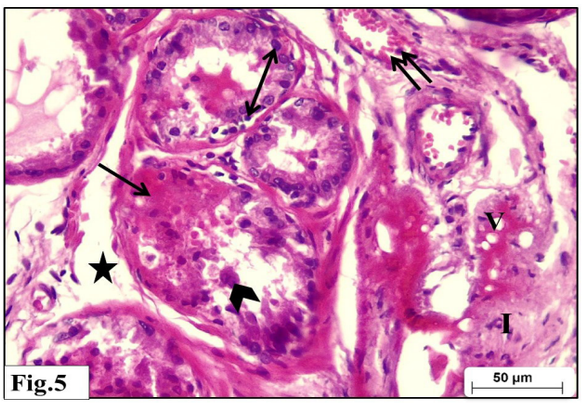

Fig. 5: A photomicrograph of a section of rat prostate gland from ZnNPs group (group II) showing some prostatic acini have marked degeneration of their lining epithelium (arrow). Some degenerated cells are shedding in the lumen (arrowhead) and others have small pyknotic nuclei (double head arrow). Notice thickening of the surrounding stroma (asterisk), monocellular inflammatory cells (I), vacuolation (V), and congested blood vessels (double arrow). H&E x 400

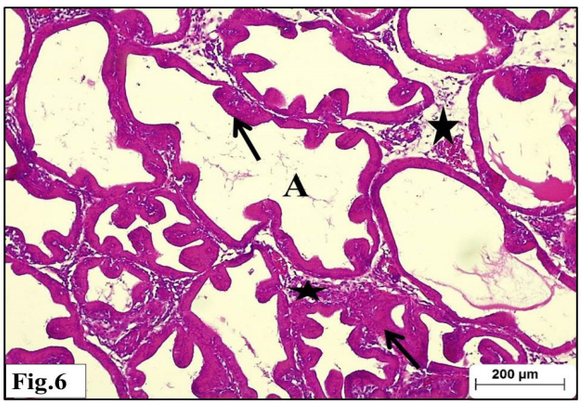

Fig. 6: A photomicrograph of a section of rat prostate gland from ZnNPs-Rutin group (group IV) showing prostatic acini (A) with slight variability in size and shape. Fibromuscular stroma (asterisk) between acini decreased in thickness. An area of hyperplasia is observed (arrow). H&E x 100

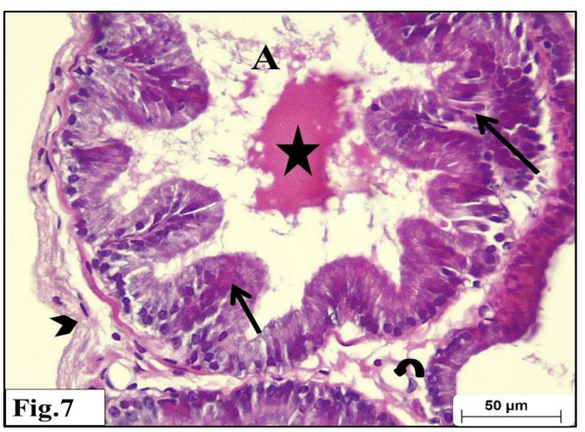

Fig. 7: A Photomicrograph of a section of rat prostate gland from ZnNPs-Rutin group (group IV) showing a prostatic acinus (A) containing shrunken prostatic secretion (asterisk) with areas of hyperplasia (arrow). The surrounding stroma is apparently normal in thickness (arrowhead) with no vacuolation or congested blood vessels (curved arrow). H&E x 400

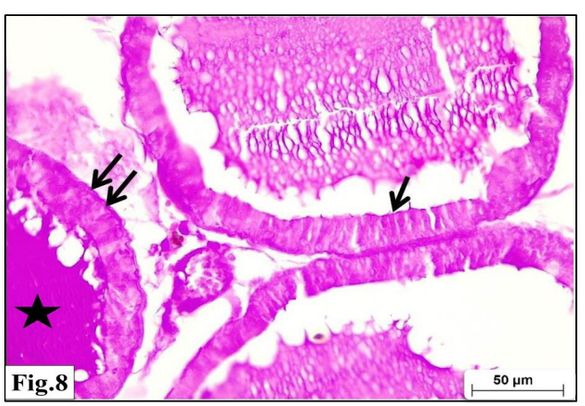

Fig. 8: A photomicrograph of a section of rat prostate gland from the control group (group I) showing PAS- positive in the epithelial lining (arrow), prostatic secretions (asterisk), and the basement membrane (double arrow). PAS x400

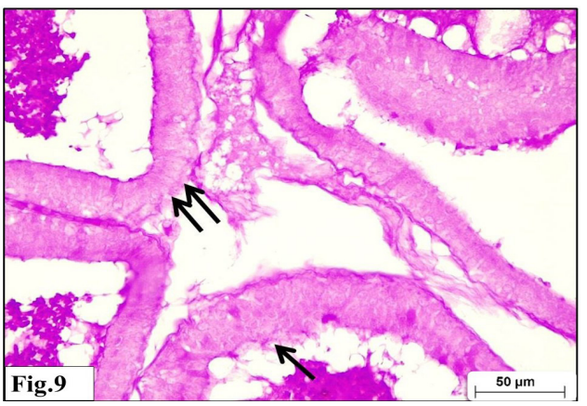

Fig. 9: A photomicrograph of a section of rat prostate gland from ZnNPs group (group II) showing a weak PAS-positive reaction in the epithelial lining (arrow) and basement membrane (double arrow). PAS x400

Fig. 10: A Photomicrograph of a section of rat prostate gland from ZnNPs-Rutin group (group IV) showing PAS-positive reaction in the epithelial lining (arrow) and basement membrane (double arrow). PAS x400

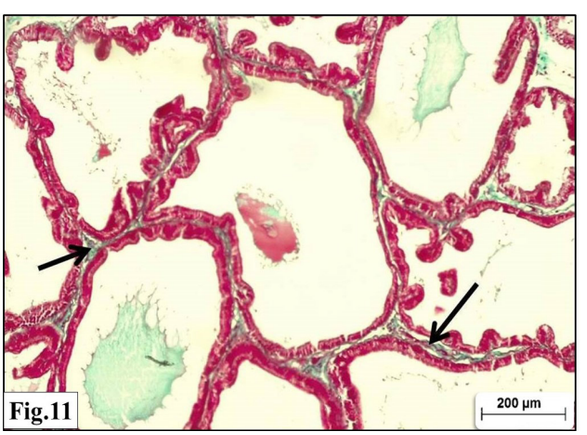

Fig. 11: A photomicrograph of a section of rat prostate gland from the control group (group I) showing a minimal amount of collagen fibers (arrow) between the prostatic acini. Masson trichrome x100

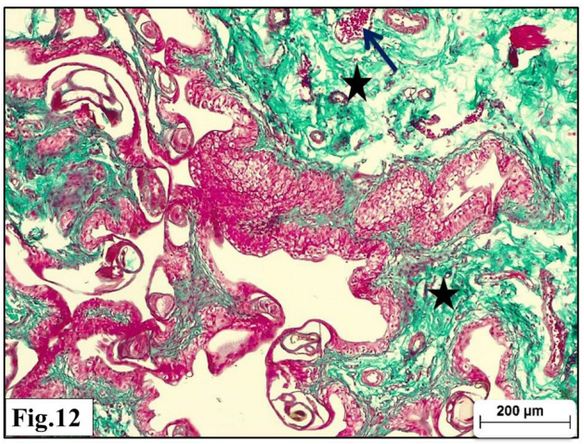

Fig. 12: A photomicrograph of a section of rat prostate gland from ZnNPs group (group II) showing the abundant amount of collagen fibers (asterisk) between prostatic acini and around congested blood vessels (arrow) Masson Trichrome x100

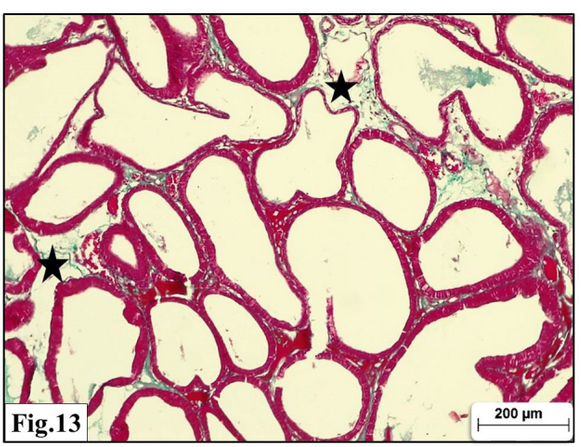

Fig. 13: A Photomicrograph of a section of rat prostate gland from ZnNPs-Rutin group (group IV) showing the apparent little amount of collagen fibers (asterisk) between prostatic acini and around blood vessels. Masson Trichrome x100

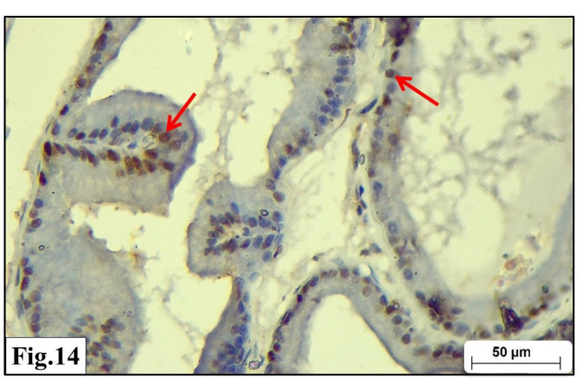

Fig. 14: A photomicrograph of a section of rat prostate gland from the control group (group I) showing positive PCNA immunoreactions in few nuclei of the lining epithelium (arrows). PCNA x400

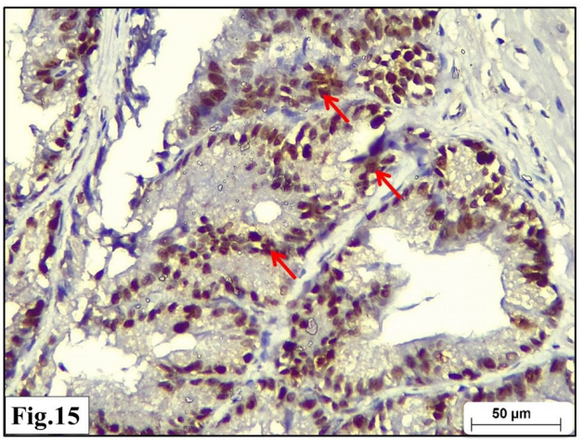

Fig. 15: A photomicrograph of a section of rat prostate gland from ZnNPs group (group II) showing intense nuclear PCNA immunoreactions in many nuclei of the lining epithelium. PCNA x400

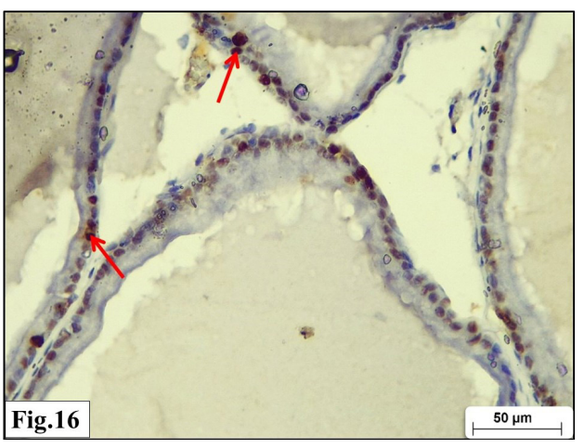

Fig. 16: A Photomicrograph of a section of rat prostate gland from ZnNPs-Rutin group (group IV) showing nuclear PCNA immunoreactions (arrow) in some nuclei of the lining epithelium. PCNA x400

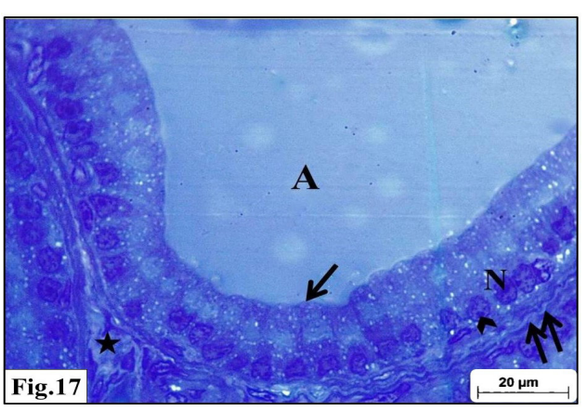

Fig. 17: A semithin section of rat prostate gland from the control group showing prostatic acini (A) lined by tall columnar epithelium (arrow) containing basal vesicular nuclei (N) with prominent nucleoli (arrowhead). Notice a prominent basement membrane (double arrow) and fibromuscular stroma (asterisk). Toluidine blue; X1000

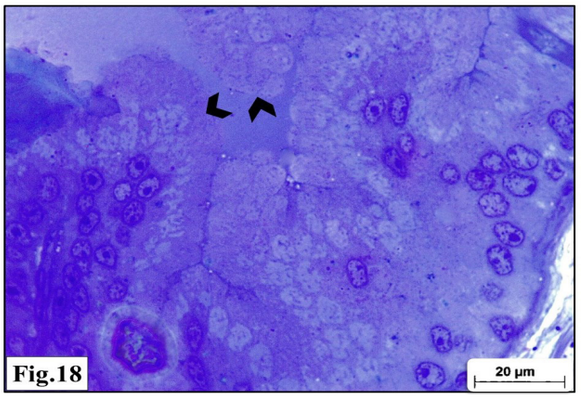

Fig. 18: A semithin section of rat prostate gland from ZnNPs group (group II) showing hyperplasia of acinar epithelial cells (arrowhead). Toluidine blue X1000

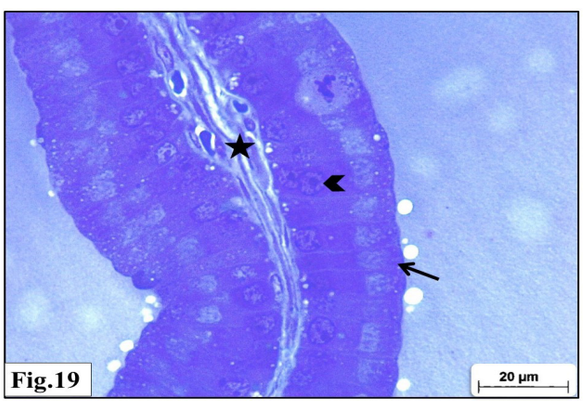

Fig. 19: A semithin section of rat prostate gland from ZnNPs-Rutin group (group IV) showing prostatic acini lined by columnar epithelium (arrow) separated by fibromuscular stroma (asterisk). Some nuclei showing mitotic figures arrowhead. Toluidine blue; X1000

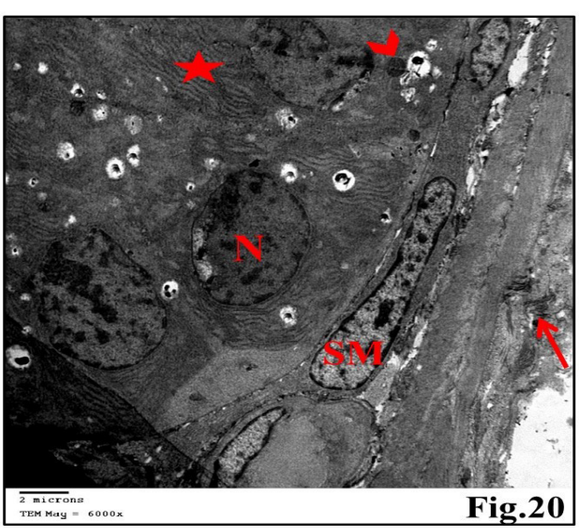

Fig. 20: Transmission electron micrograph of a section of rat prostate gland from the control group (group I) showing prostatic acinar cell having a basal euchromatic nucleus (N) and their cytoplasm contains rough endoplasmic reticulum (asterisk) and mitochondria (arrowhead). The acinar cell is resting on a regular basement membrane which is surrounded by a thick connective tissue capsule (arrow) with smooth muscle fibers (SM). TEM X 6000

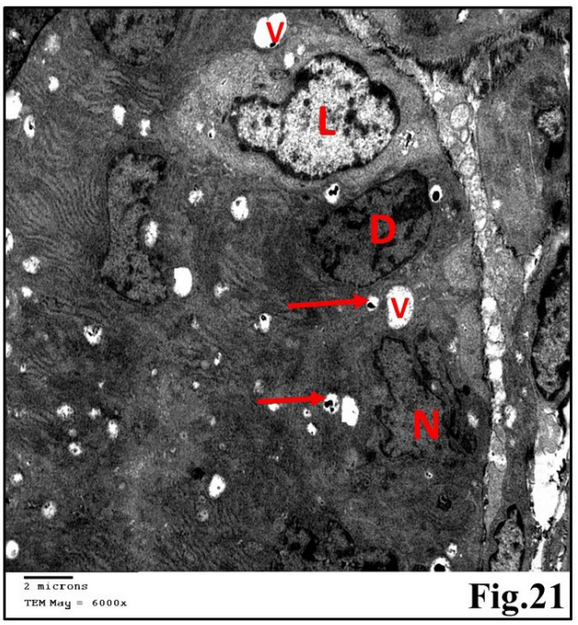

Fig. 21: Transmission electron micrograph of a section of rat prostate gland from ZnNPs group (group II) showing some of the acinar cells are electron lucent with irregular nuclei (L) and others are electron-dense with regular nucleus (D). Their cytoplasm contains vacuolation (V) and vacuoles contain electron-dense structures inside the acinar cells (arrow). Notice irregular bilobed nucleus (N). TEM X 6000

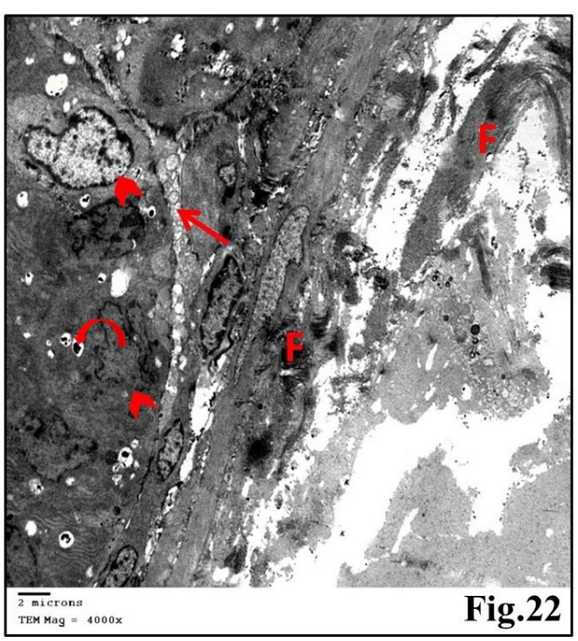

Fig. 22: Transmission electron micrograph of a section of rat prostate gland from ZnNPs group (group II) showing separation between acinar cells and basement membrane (arrow). Bundles of collagen fibers of different directions (F) in the basement membrane and irregular nuclear membrane (arrowhead) are observed. There are vacuoles contain electron-dense structure inside the acinar cells (curved arrow). TEM X 4000

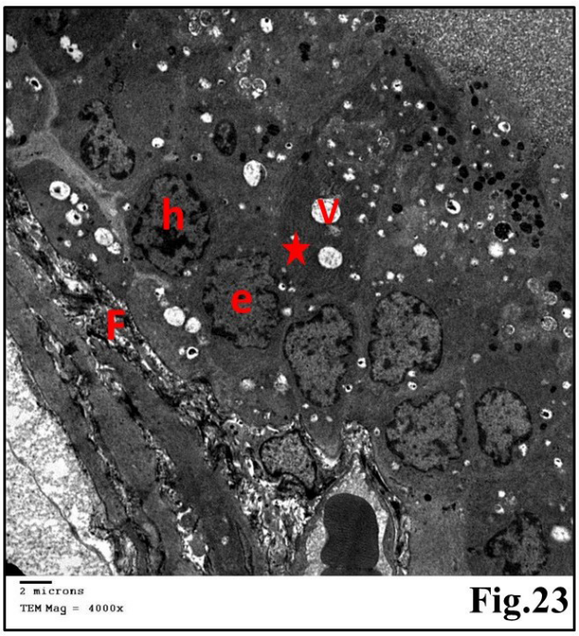

Fig. 23: Transmission electron micrograph of a section of rat prostate gland from ZnNPs-Rutin group (group IV) showing the cytoplasm of all cells is the same in electron densities but the nuclei contain euchromatin (e) and heterochromatin (h). Their cytoplasm contains vacuolation (V), rough endoplasmic reticulum (asterisk). Notice the apparent decrease in the amount of fibrous tissue (F) in the basement membrane. TEM X 4000

Table 1: Effect of Rutin treatment on the MDA, PSA levels in the studied groups of animals after prostate damage by ZnNPs (Mean ± SD)

Parameters	G I	G II	G III	G IV
MDA (nmol/mg)	1.703±0.2776	3.325±0.4098	1.785±0.4454	2.385±0.442
PSA (ng/ml)	0.15±0.026	0.35±0.0433	0.17±0.026	0.13±0.014

Table 2: Effect of Rutin treatment on the structure of prostate gland in the studied groups of animals after prostate damage by ZnNPs (Mean ± SD)

Parameters	G I	G II	G III	G IV
Relative-organ weight	0.3003±0.015	0.3606±0.1162	0.302±0.021	0.289±0.0078
Area of ٪ of collagen fibers	0.015±0.0026	14.872±4.0126	0.014±0.0033	0.019±0.003
Mean number of PCNA positive cells	16.33± 3.326	36.33±5.006	17.5±2.429	21.17±5.193

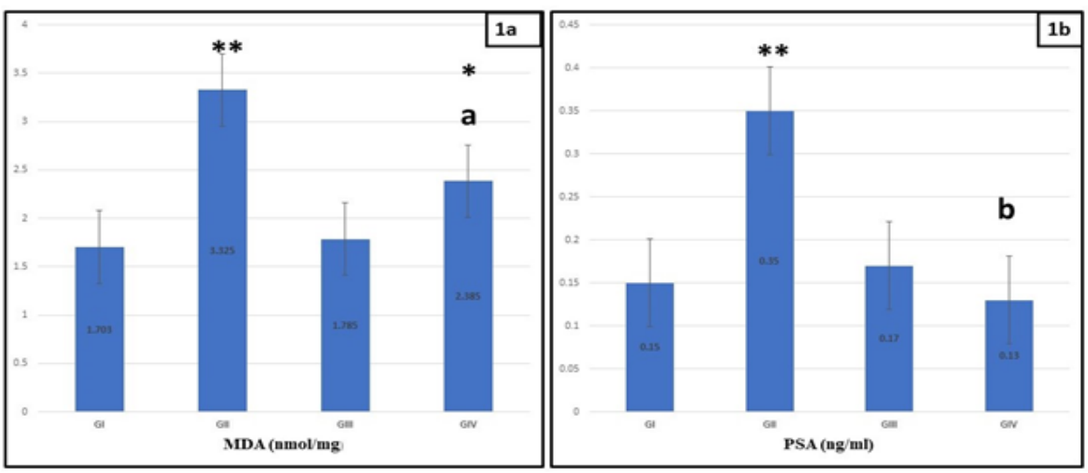

Histogram 1: Effect of Rutin treatment on the MDA, PSA levels in the studied groups of animals after prostate damage by ZnNPs. All data represented as mean ± SEM. (*, ** = statistically ($p < 0:05$) and highly statistically ($p < 0.001$) versus control group, respectively) (a, b= statistically ($p < 0.05$) and highly statistically significant respectively, versus ZnNPs group ($p < 0:001$)). Data were analyzed by one-way ANOVA using Tukey's post hoc test.

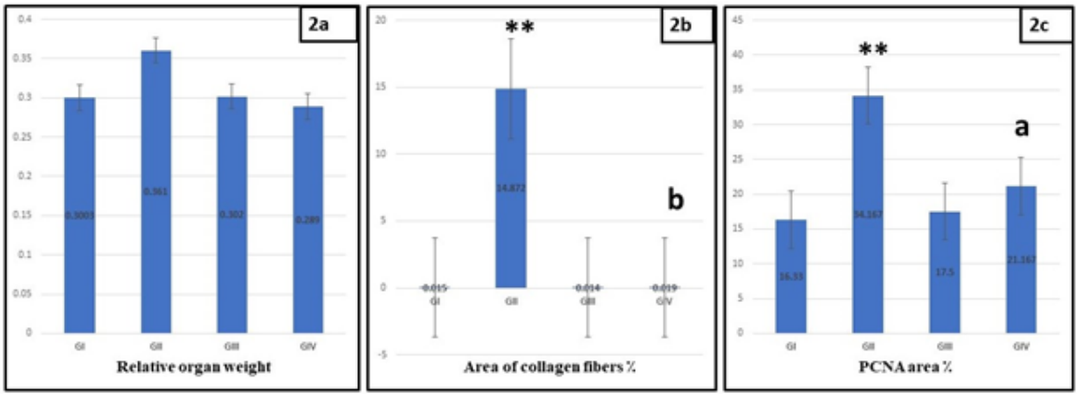

Histogram 2: Effect of Rutin treatment on the structure of prostate gland in the studied groups of animals after prostate damage by ZnNPs. All data represented as mean ± SEM. (** = highly statistically ($p < 0.001$) versus control group) (a, b = statistically ($p < 0.05$) and highly statistically ($p < 0.001$) respectively, versus ZnNPs group). Data were analyzed by one-way ANOVA using Tukey's post hoc test.

DISCUSSION

The safety and risk effects of ZnNPs on different tissues have been a challenge for a lot of research recently[23]. Despite the increased application of zinc nanoparticles in biomedicine, it was suspected to cause cytotoxicity on various human cells which might be time and dose-dependent[24,25,26]. The present study investigates the toxic effects of Zn NPs on the cells of the prostate gland in adult rats using light and electron microscopic examination.

Group II (ZnNPs group) in the current study showed an insignificant increase in ROW in comparison to the control group. However, the authors previously suggested that the imbalance between cell pro¬liferation and apoptosis can lead to augmentation in prostate gland weight[27]. Chen *et al*.[28] stated that organ weight is the most sensitive and common indicator of the harmful effects of drugs on animals. Also, the blood-PSA concentration, in our study, showed a highly statistically significant increase in comparison to the control group which could be explained by the fact that the increase in PSA is a risk factor in the genesis and progression of prostate tumors[29].

In the current study, light microscopic findings of rats' prostatic cells that received ZnNPs, revealed histological changes in the prostatic epithelium. Distortion and coalesce of the acini made it resemble benign nodular hyperplasia with the appearance of areas of vacuolation in prostatic secretions. Such findings could be correlated to the imbalance between oxidants and antioxidants leading to free-radical production and excess reactive oxygen species (ROS) that predispose to oxidative stress and tissue damage mentioned in previous research[20,27]. This ROS production associated with ZnNPs resulted in inhibition of vital enzymes with an increase in DNA double-strand breakage and penetration of the cell membrane. Previous data suggested that the relationship between prostatic hyperplasia and the inflammation of the prostate with subsequent tissue damage and trials of healing might be the cause of nodule development[30].

In the present study, MDA which is a marker of oxidative stress and lipid per¬oxidation showed a highly statistically significant increase in group II (ZnNP group) in comparison to the control group. Authors previously explained that an increase in MDA is related to oxidative stress and damaged proteins and/or lipids normally present in the cell membrane. The increase in MDA reflects the increased production of ROS with its subsequent inflammatory and cytotoxic events[18]. Other authors added that there is a reverse relationship between ZnNPs size and the inflammatory response, toxicity, and induction of apoptosis. The size of the nanoparticles and their surface area hugely influence their capacity to produce ROS and consequently yield their cellular toxicity[31].

Previous studies detected that the application of ZnNPs could lead to suppurative inflammation in the prostate gland due to continuous irritation of cells by oxidative stress[31] that might explain the pink hyaline plaques and detachment of the epithelium of our current study. This goes following the findings that oxidative damage causes the desquamation of glandular epithelial cells[18]. The degeneration of epithelium with pyknotic nuclei was reinforced by the decrease in the PAS-positive reaction in the epithelium. The epithelium injury triggers cell differentiation by mitosis that leads to the growth of a new hyperplastic epithelium[20,32].

Congestion of the blood vessels seen in the current study could be a reaction of the cells to increase their oxygen supply in a trial to restore the oxygen ratio to the normal level[32]. Both Masson trichrome stained sections examination and morphometric analysis revealed a highly statistically significant increase in the area percent of collagen fibers as elaborated previously that oxidative stress leads to the overproduction of collagen and fibrosis[31].

A highly statistically significant increase in the PCNA positive immunohistochemical reactions was detected in the nuclei of the glandular epithelium. PCNA plays an

important role in DNA replication and other associated processes thus regulating various cell activities[33]. Any disturbance in DNA function might contribute to the irregularity of nuclear membranes seen in the semithin sections of rats' prostate cells receiving ZnNPs in the present work.

Electron microscopic study expanded on the findings of the light microscope with the cell cytoplasm showing vacuolations. Similar ultrastructural findings were seen after various chemical injury exposures in adult male albino rats. Authors suggested that these degenerative epithelial changes could be attributed to oxidative stress which was marked by the significant decrease in the prostatic glutathione level[34].

Many food supplements and plant-derived bioactive material have been introduced for the treatment of several diseases that might result from oxidative stress after exposure to metallic hazards. These trends have rendered positive results[35]. Rutin has been used in multifunctional effects on the various cellular elements especially those under some pathological conditions[36]. Dietary contents of such flavonoid material help develop and proper function of the immune system[37].

In this research, the protection of prostate cells, using Rutin, against the toxicity of ZnNPs was attempted with satisfactory results. Group IV examined cells (ZnNPs+ Rutin), in the current study, showed a statistically significant decrease in MDA level in comparison to Group II; thus, manifesting on the antioxidant effects of Rutin.

Rutin has a strong antioxidant activity that scavenger oxygen and nitrogen free radicals and inhibits lipid peroxidation[15,36]. Any diet containing Rutin could be of important use for the dysfunction in the reproductive activities in males through decreasing lipid peroxidation and oxygen-free radicals[38].

Prostate cells of rats subjected to ZnNPs and Rutin showed diminished nanoparticle-induced changes and appeared more or less as the control. The histological findings were augmented by the special staining techniques of PAS, Masson Trichrome methods, PCNA, and morphometric studies. ROW in group IV showed a non-statistically significant decrease in comparison to the group I and PSA showed a highly statistically significant decrease in comparison to group I. This might imply that Rutin administration has natural effects on the tissues with no risks for usage and it is capable of oxidizing lipid peroxidation as well as chelating of metal ions. This advocates the probable role of its dietary intake to lower some pathological hazards[13].

Rutin, which is found in many foods like onions, apples, and citrus fruits, was found to inhibit mitochondrial dysfunction, the stress of the endoplasmic reticulum, oxidative stress as well as other metabolic functions thus ameliorating inflammation and lipid accumulation which proposes its effectiveness in chronic metabolic diseases[39]. Also, Rutin was reported to have an amelioration response on the reproductive organs of male rats subjected to cyclophosphamide-induced toxicity particularly on the testis and epididymis cells which were mainly reflected in the sperm count, motility, and abnormal sperm morphology[40].

Although some residual effects of toxicity of ZnNPs on the protected group with Rutin still exist in our current study, this might suggest that Rutin's protective effects are dose or time-dependent. A more experimental time or increased doses of Rutin intake can increase the satisfactory effects of its protective role. However, Rutin is expected to become a new rival medication in protecting tissues against certain inflammatory conditions through safeguarding human cells from the damage caused by tumor necrotizing factor-alpha[41].

CONCLUSION

The current study concludes that exposure to Zinc nanoparticles had some histopathological and biochemical changes on cells of the prostate gland. Meanwhile, Rutin, with its known antioxidant properties, was able to protect these cells from such toxic effects which could reflect on male fertility problems especially for those continuously exposed to such metallic hazards. More emphasis is still needed on its dose and time-dependent protective effects.

CONFLICT OF INTERESTS

There are no conflicts of interest.

REFERENCES

1. Elshama SS, El-kenawy AE, Osman HH. Histopathological study of zinc oxide nanoparticle-induced neurotoxicity in rats. Current Topics in Toxicology 2017;13:95–103.

2. Shim KH, Jeong K, An SSA. Assessment of ZnO and SiO 2 nanoparticle permeability through and toxicity to the blood – brain barrier using Evans blue and TEM. International Journal of Nanomedicine 2014;9:225–33.

3. Remzova M, Zouzelka R, Brzicova T, Vrbova K, Pinkas D, Rőssner P, *et al*. Toxicity of TiO2, ZnO, and SiO2 nanoparticles in human lung cells: Safe-by-design development of construction materials. Nanomaterials 2019;9.

4. Reza EH, Mohammad F, Leila S, Babadi Y, Bakhshiani V. Investigation the Zinc Oxide Nanoparticle ' s Effect on Sex Hormones and Cholesterol in Rat. International Research Journal of Biological Sciences 2013;2:54–8.

5. Varzeghani SM, Parivar K, Abdollahifar M-A, Karamian A. Effects of Iron Oxide Nanoparticles on Mouse Sperm Parameters and Testicular Tissue. Iranian Journal of Toxicology 2018;12:39–44.

6. Rollerova E, Jurcovicova J, Mlynarcikova A, Sadlonova I, Bilanicova D, Wsolova L, *et al*. Delayed adverse effects of neonatal exposure to polymeric nanoparticle poly(ethylene glycol)-block-polylactide methyl ether on hypothalamic-pituitary-ovarian axis development and function in Wistar rats. Reproductive Toxicology 2015;57:165–75.
7. Hussein MMA, Ali HA, Saadeldin IM, Ahmed MM. Querectin Alleviates Zinc Oxide Nanoreprotoxicity in Male Albino Rats. Journal of Biochemical and Molecular Toxicology 2016;30:489–96.
8. Motrich RD, Salazar FC, Breser ML, Oberti JPM, Godoy GJ, Olivera C, *et al*. Implications of prostate inflammation on male fertility. Andrologia 2018;50:e13093.
9. Kim YR, Park J Il, Lee EJ, Park SH, Seong NW, Kim JH, *et al*. Toxicity of 100 nm zinc oxide nanoparticles: A report of 90-day repeated oral administration in Sprague Dawley rats. International Journal of Nanomedicine 2014;9:109–26.
10. Namvar F, Rahman HS, Mohamad R, Azizi S, Tahir PM, Chartrand MS, *et al*. Cytotoxic Effects of Biosynthesized Zinc Oxide Nanoparticles on Murine Cell Lines. Evidence-Based Complementary and Alternative Medicine 2015;2015:593014.
11. Abarikwu SO, Olufemi PD, Lawrence CJ, Wekere FC, Ochulor AC, Barikuma AM. Rutin, an antioxidant flavonoid, induces glutathione and glutathione peroxidase activities to protect against ethanol effects in cadmium-induced oxidative stress in the testis of adult rats. Andrologia 2017;49:1–12.
12. A U, Z Z, KH C, NA N, Z AM. Role of rutin on nitric oxide synthesis in human umbilical vein endothelial cells. Scientific World Journal 2014;2014:169370.
13. Khan RA, Rashid Khan M, Ahmed M, Shah MS, Rehman SU, Khan J, *et al*. Effects of rutin on testicular antioxidant enzymes and lipid peroxidation in rats. Indian Journal of Pharmaceutical Education and Research 2017;51:412–7.
14. Ganeshpurkar A, Saluja AK. The Pharmacological Potential of Rutin. Saudi Pharmaceutical Journal 2017;25:149–64.
15. Jahan S, Munawar A, Razak S, Anam S, Ain QU, Ullah H, *et al*. Ameliorative effects of rutin against cisplatin-induced reproductive toxicity in male rats. BMC Urology 2018;18:1–11.
16. Abdel-Aziz MM, Yosri M, Amin BH. Control of imipenem resistant -Klebsiella pneumoniae pulmonary infection by oral treatment using a combination of mycosynthesized Ag-nanoparticles and imipenem. Journal of Radiation Research and Applied Sciences 2017;10:353–60.
17. Hejazy M, Koohi MK. Effects of Nano-zinc on Biochemical Parameters in Cadmium-Exposed Rats. Biological Trace Element Research 2017;180:265–74.
18. Ibrahim W, Oda S, Khafaga A. Pathological Evaluation of The Effect of Zinc Oxide Nanoparticles on Chromium-Induced Reproductive Toxicity in Male Albino Rats. Alexandria Journal of Veterinary Sciences 2017;53:24.
19. Suvarna SK, Layton C, Bancroft JD. Bancroft's theory and practice of histological techniques, 7th edition .Elsevier Health sciences, Churchill Livingstone. 2013.
20. Sakr SA, Mahran HA, Nofal AE. Effect of Selenium on Carbimazole-Induced Histopathological and Histochemical Alterations in Prostate of Albino Rats. American Journal of Medicine and Medical Sciences 2012;2:5–11.
21. Farag EA, Yousry MM. Effect of mobile phone electromagnetic waves on rat testis and the possible ameliorating role of Naringenin : A histological study. Egyptian Journal of Histology 2017;41:108–21.
22. Bhutia Y, Ghosh A, Sherpa ML, Pal R, Mohanta PK. Serum malondialdehyde level: Surrogate stress marker in the Sikkimese diabetics. Journal of Natural Science, Biology and Medicine 2011;2:107–12.
23. Mohammad GR, Karimi E, Oskoueian E, Homayouni-Tabrizi M. Anticancer properties of green-synthesised zinc oxide nanoparticles using Hyssopus officinalis extract on prostate carcinoma cells and its effects on testicular damage and spermatogenesis in Balb/C mice. Andrologia 2020;52:e13450.
24. Fu J, Zeng X, He N. Comparative cytotoxicity induced by zinc oxide nanoparticles in human prostate cells. Journal of Nanoscience and Nanotechnology 2017;17:196–202.
25. Hejazy M, Koohi MK. Effect of sub acute exposure of nano Zinc particles on oxidative stress parameters in rats. Iranian Journal of Veterinary Medicine 2017;11:155–64.
26. Pinho AR, Rebelo S, de Lourdes Pereira M. The impact of zinc oxide nanoparticles on male (In) fertility. Materials 2020;13:1–18.
27. Sarbishegi M, Khani M, Salimi S, Valizadeh M, Aval FS. Antiproliferative and antioxidant effects of withania coagulans extract on benign prostatic hyperplasia in rats. Nephro-Urology Monthly 2016;8:1–7.
28. Chen B, Hong W, Yang P, Tang Y, Zhao Y, Aguilar ZP, *et al*. Nano zinc oxide induced fetal mice growth restriction, based on oxide stress and endoplasmic reticulum stress. Nanomaterials 2020;10:259.

29. Berroukche A, Terras M, Labani A, Dellaoui H, Lansari W. Effects of interaction Cd[sbnd]Zn on serum-PSA level and prostate histology in rats. Asian Pacific Journal of Tropical Biomedicine 2017;7:245–8.

30. De Nunzio C, Presicce F, Tubaro A. Inflammatory mediators in the development and progression of benign prostatic hyperplasia. Nature Reviews Urology 2016;13:613–26.

31. Mesallam DI., Deraz RH, Abdel Aal SM, Ahmed SM. Toxicity of Subacute Oral Zinc Oxide Nanoparticles on Testes and Prostate of Adult Albino Rats and Role of Recovery. Journal of Histology and Histopathology 2019;6:2.

32. Tolba AM, Mandour DA. Histological effects of bisphenol-A on the reproductive organs of the adult male albino rat. European Journal of Anatomy 2018;22:89–102.

33. Boehm EM, Gildenberg MS, Washington MT. The Many Roles of PCNA in Eukaryotic DNA Replication. Enzymes 2016;39:231–54.

34. Hashem HE, Abd El-Haleem MR, Abass MA. Epithelial and stromal alterations in prostate after cypermethrin administration in adult albino rats (histological and biochemical study). Tissue and Cell 2015;47:366–72.

35. Enogieru AB, Haylett W, Hiss DC, Bardien S, Ekpo OE. Rutin as a potent antioxidant: Implications for neurodegenerative disorders. Oxidative Medicine and Cellular Longevity 2018;2018:6241017.

36. Budzynska B, Faggio C, Kruk-Slomka M, Samec D, Nabavi SF, Sureda A, *et al*. Rutin as Neuroprotective Agent: From Bench to Bedside. Current Medicinal Chemistry 2019;26:5152–64.

37. Ganeshpurkar A, Saluja AK. Protective effect of rutin on humoral and cell mediated immunity in rat model. Chemico-Biological Interactions 2017;273:154–9.

38. Qu S, Dai C, Guo H, Wang C, Hao Z, Tang Q, *et al*. Rutin attenuates vancomycin-induced renal tubular cell apoptosis via suppression of apoptosis, mitochondrial dysfunction, and oxidative stress. Phytotherapy Research 2019;33:2056–63.

39. Li T, Chen S, Feng T, Dong J, Li Y, Li H. Rutin protects against aging-related metabolic dysfunction. Food and Function 2016;7:1147–54.

40. Abarikwu SO, Otuechere CA, Ekor M, Monwuba K, Osobu D. Rutin ameliorates cyclophosphamide-induced reproductive toxicity in male rats. Toxicology International 2012;19:207–14.

41. Zhao B, Zhang W, Xiong Y, Zhang Y, Jia L, Xu X. Rutin protects human periodontal ligament stem cells from TNF-α induced damage to osteogenic differentiation through suppressing mTOR signaling pathway in inflammatory environment. Archives of Oral Biology 2020;109:104584.

الملخص العربى

التغييرات الخلوية والكيميائية المستحدثة بجزيئات الزنك المتناهية الصغر في غدة البروستات للجرذان البيضاء البالغة والدور الوقائي المحتمل للروتين

هبه رمضان هاشم، مريم أسعد أمين

قسم التشريح وعلم الأجنة، كلية الطب، جامعة عين شمس، القاهرة، مصر

المقدمة: تستخدم جزيئات الزنك المتناهية الصغر في عديد من المجالات الطبية والصناعية. ولكن مؤخرا ظهرت تقارير عن تأثيرها الضار. الروتين هو فلافينويد موجود في النباتات والعديد من الخضروات والفواكه ويعتبر من مضادات الاكسدة القوية.

الهدف: الكشف عن التأثير السام لجزيئات الزنك المتناهية الصغر علي غدة البروستات للجرذان البيضاء البالغة والتقييم للتأثير الوقائي المحتمل للروتين.

المواد والطرق: تم تقسيم خمسون من ذكور الجرذان البيضاء البالغة إلى أربع مجموعات. المجموعة الأولي: كمجموعة ضابطة، المجموعة الثانية: تم حقن الجرذان بجزيئات الزنك المتناهية الصغر ١٠٠ مجم/ كجم عن طريق الفم لمدة ٢٨ يوما. المجموعة الثالثة: تم حقن الجرذان بالروتين ٥٠ مجم/ كجم عن طريق الفم لمدة ٢٨ يوما.المجموعة الرابعة: تم حقن الجرذان بجزيئات الزنك المتناهية الصغر و الروتين بنفس الجرعة وطريقة المجموعات السابقة. بعد ٢٨ يوما، تم وزن الفئران وسحب عينات الدم ثم التضحية بها. تم تشريح غدة البروستاتا ومعالجتها من أجل الفحص المجهري والنسيجي المناعي والفحص المجهري الدقيق مع التحليلات البيوكيميائية والمورفومترية.

النتائج: أظهر الفحص المجهري لعينات المجموعة الثانية خلل في تناسق الحويصلات وإنحطاطها والتسلل الخلوي. لوحظ نقص في صبغة حمض شيف الأيودي وزيادة بسماكة السدى الليفي العضلي في عينات مالوري ثلاثي الألوان. وجد زيادة بالصبغة الهستوكيميائية المناعية في الظهارة الغدية. أظهر الفحص بالمجهر الالكتروني الدقيق نقص في عدد الحبيبات الإفرازية وإتساع الشبكة الإندوبلازمية الخشنة في سيتوبلازم الخلايا. يصاحب هذه النتائج زيادة ذات دلاله إحصائية في الـ MDA, PSA وزيادة في الوزن النسبي للعضو. علي العكس من ذلك, أظهرت عينات المجموعة الرابعة إستعادة لترتيب خلايا البروستاتا مع وجود مناطق متضخمة و نقص ذات دلالة إحصائية في ال MDA, PSA.

الإستنتاج: أثبتت هذه النتائج أن الروتين له دور وقائي طبيعي ضد الإصابة التي أحدثتها جزيئات الزنك المتناهية الصغر بخلايا البروستاتا في الجرذان.